Electrical spin injection in metallic mesoscopic spin valves

Jedema, Friso

Chapter 4

Magnetization reversal processes in rectangular ferromagnetic strips

4.1 Introduction

The resistance of a single Py, Co or Ni strip is a few percent smaller when the magnetization direction is perpendicular to the current direction as compared to a parallel alignment. This effect is known as the anisotropic magnetoresistance (AMR) effect [1]. The AMR effect can therefore be used to monitor the magnetization reversal or 'switching' behavior of the ferromagnetic Py, Co and Ni electrodes [2]. Three different models are discussed here which describe the magnetization reversal processes in mesoscopic strips [3]. Their applicability depends on the dimensions of the magnetic strip and its material properties such as the saturation magnetization M_s, the crystalline anisotropy contants K_1, K_2,..., and the exchange constant A. For elongated particles as the ferromagnetic strips used in this thesis, non-uniform magnetization reversal processes are most likely to be present as the width of the strip always largely exceeds the (magnetic) exchange length $\lambda_{ex} = \sqrt{4\pi A/\mu_0 M_S^2}$, being $\approx$ 6 nm, $\approx$ 7 nm and $\approx$ 21 nm for Fe, Co and Ni respectively [3].

4.2 Magnetization reversal via uniform rotation

The simplest description is provided by the Stoner and Wohlfarth model (SW) [4]. It assumes a single ferromagnetic domain and coherent magnetization rotation. Neglecting the magneto-crystalline anisotropy, the total energy for an ellipsoid of revolution is written as a sum of magnetostatic and shape anisotropy energies:

$$E = -\mu_0 H M_s cos\phi - \frac{\mu_0 M_s^2}{2}(D_z - D_x)\cos^2(\phi - \theta)\ , \qquad (4.1)$$

where M_s is the saturation magnetization, D_z and D_x are the demagnetization factors, and ϕ and θ are the angles between the magnetization direction and the applied field, and, respectively, the external field and the easy axis. The second term on the right of eq. 4.1 represents the shape anistropy energy of the ellipsoid, which is equal to the magnetostatic self-energy of the particle. For an elongated ellipsoid along the z-axis the demagnetization factors would be $D_x = 0.5$, $D_y = 0.5$ and $D_z = 0$. The angle between the magnetization and the applied field for a given field can be determined analytically by minimizing the total energy. The switching or coercive field as a function of the direction of the applied field reads:

$$H_c(\theta) = H_0^{sw}(\sin^{2/3}\theta + \cos^{2/3}\theta)^{-3/2} \ , \tag{4.2}$$

where $H_0^{sw} = M_s(D_z - D_x)$ is the saturation field in perpendicular ($\theta = 90°$) direction, which corresponds to the demagnetization field along the (short) x-axis of the ellipsoid of revolution. An upper value estimate is therefore obtained of the switching field for a permalloy ellipsoid of $\mu_0 H_0^{sw} = 540\ mT$, using $M_s = \ 8.6 \cdot 10^5\ A/m$, whereas for a Co ellipsoid $\mu_0 H_0^{sw} = 900\ mT$ is obtained, using $M_s = \ 1.4 \cdot 10^6\ A/m$. In Fig. 4.1a and 4.2a the saturation field is indicated by $B_0^{sw} = \mu_0 H_0^{sw}$ for Py and Co rectangular strips. Here the saturation fields are less than the maximal upper value, due smaller demagnetization factors for the rectangular Py and Co bars [5].

However for fields applied parallel to the easy axis ($\theta = 0$) of a mesoscopic strip, it was found that the switching field is one order of magnitude smaller than the SW-model predicts [6–12]. To explain these low switching fields another switching mechanism have been proposed: a magnetization curling process.

The curling model assumes that the magnetization direction rotates in a plane perpendicular to the anisotropy axis of the wire, effectively reducing the longitudinal component of the magnetization and hence the magnitude of the switching field [13–15]. For rectangular shaped strips, the upper and lower bound of the magnitude of the switching field have been calculated for a B-field applied parallel to the easy axis ($\theta = 0°$) of the strip. For aspect ratios $d/h < 4$, where $2d$ is width and $2h$ is the height of the strip, these upper and lower bounds are the same. The magnitude of the switching field, as calculated by Aharoni, can then be written as [14]:

$$H_c^{curl}(0°) = \frac{\pi}{2} M_s \frac{\lambda_{ex}^2}{d^2} \ . \tag{4.3}$$

For permalloy one finds that $\lambda_{ex} \approx 12$ nm, using $A = \ 1 \cdot 10^{-11}\ J/m$ and $M_s = \ 860\ kA/m$. For a 100 nm wide rectangular Py electrode and a field applied parallel to the long (easy) axis, a switching field of $\mu_0 H_c^{curl}(0°) = \ 91$ mT would thus be obtained.

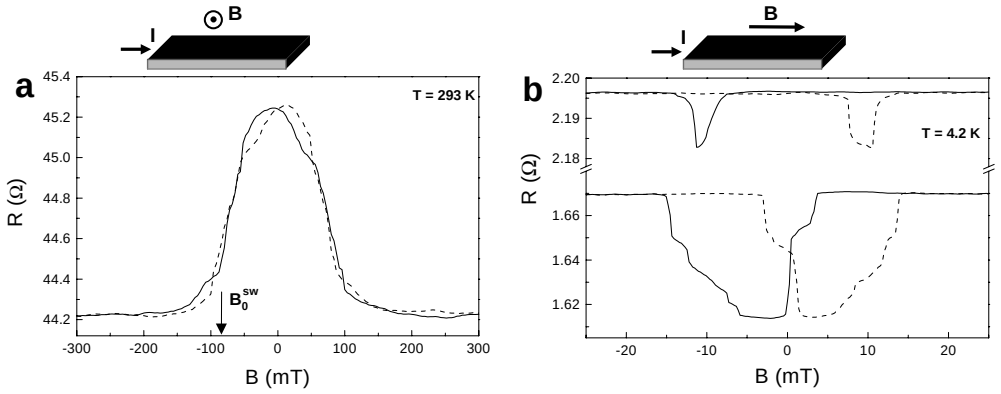

Figure 4.1: *(a) Typical AMR curve at RT of a* $14 \times 0.5\ \mu m^2$ *Py strip with the magnetic field applied in the plane of the substrate and perpendicular to the current. (b) AMR behavior at* $T = 4.2\ K$ *with the magnetic field parallel to the direction of the current for two rectangular Py strips with dimensions* $2.0 \times 0.8\ \mu m^2$ *(bottom) and* $2.0 \times 0.5\ \mu m^2$ *(top). The solid (dotted) curve corresponds with a negative (positive) sweep direction of the B-field.*

4.3 Non-uniform magnetization reversal

This mechanism assumes that the switching of the magnetization is mediated by the nucleation of a domain-wall [16, 17]. A domain-wall (or more) is nucleated (annihilated) when the cost of exchange energy associated with the domain wall is lower (higher) than the gain in magnetostatic energy upon increasing the external field. Once it is nucleated it can sweep through the material, thereby lowering the total magneto static energy. This mechanism has been confirmed experimentally by Lorentz micrography by Otani [18]. Recent MFM studies of 1 μm wide iron and permalloy wires seem to indicate that in these wires a multi-domain structure is formed during the reversal process [19, 20]. However an analytical expression of the magnitude of the nucleation field cannot easily be given, as one has to numerically solve the time dependent Landau-Lifshitz equations for each value of the applied magnetic field.

4.4 The AMR behavior of rectangular Py and Co strips

Typical anisotropic magnetoresistance (AMR) curves at RT of a $14 \times 0.5\ \mu m^2$ Py strip and $0.2 \times 12\ \mu m^2$ Co strip are shown in Fig. 4.1a and Fig. 4.2a. The magnetic field in these measurements is directed perpendicular to the long axis of the strips and parallel to the substrate plane. The saturation

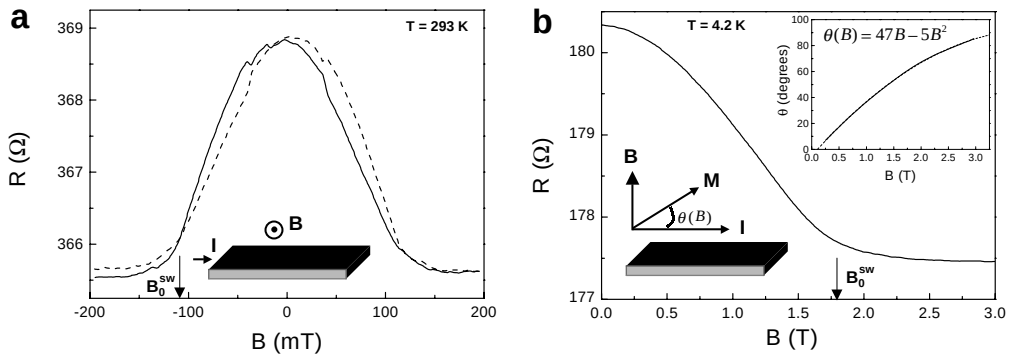

Figure 4.2: *Perpendicular AMR of a* $0.2 \times 12\ \mu m^2$ *Co electrode, (a) with the magnetic field B applied perpendicular the Co strip but parallel to the substrate plane at RT and (b) with the magnetic field B applied perpendicular to the substrate plane at* $T = 4.2$ *K. The inset in (b) shows the angle between the magnetization* $\boldsymbol{M}$ *and the direction of the current through the wire, see text.*

fields as used in the SW-model are indicated by B_0^{sw}. The 40 nm thick and 500 nm wide Py strip has a demagnetization factor in the direction of the applied magnetic field of $D \approx 0.06$ [5] and the SW-model predicts $B_0^{sw} \approx 65$ mT, which is close the observed value of around 80 mT. The 50 nm thick and 200 nm wide Co electrode has a demagnetization factor in the direction of the applied magnetic field of $D_y \approx 0.15$, yielding an expected saturation field of $B_0^{sw} \approx 270$ mT, according to the SW-model. This is more than a factor two larger than the observed value of around 110 mT. When the magnetic field is applied perpendicular to the substrate plane at $T = 4.2$ K, shown in Fig. 4.2b, a saturation field is found approximately $B_0^{sw} = 1.8$ T. The deviation from the expected SW-model saturation field at RT in Fig. 4.2a might be related by an additional anisotropy energy due to strain in the Co film, because a 2 times larger switching field at $T = 4.2$ compared to RT is also observed in the Co strips, when the magnetic field is applied parallel to the long-axis of the Co strip (see Chapter 6).

The inset of Fig. 4.2b shows the angle $\Psi(= \phi - \theta)$ as a function of the magnetic field, obtained by fitting the AMR curve of Fig. 4.2b to Eq. 2.6 and assuming that the magnetization rotation is uniform. According to the Stoner and Wohlfarth model (Eq. 4.1) for $\theta = \pi/2$, $D_z = 0$ and $D_x = 1$, the angle Ψ between the current and the magnetization direction should behave like $\Psi = \arccos(B/M_s)$. However the inset of Fig. 4.2b shows that this relation is only obeyed at low fields.

The typical AMR behavior at $T =$ 4.2 K with the magnetic field directed parallel to the direction of the current ($\theta = 0°$) is shown in Fig. 4.1b for rectangular $2.0 \times 0.8\ \mu m^2$ (bottom curves) and $2.0 \times 0.5\ \mu m^2$ (top curves)

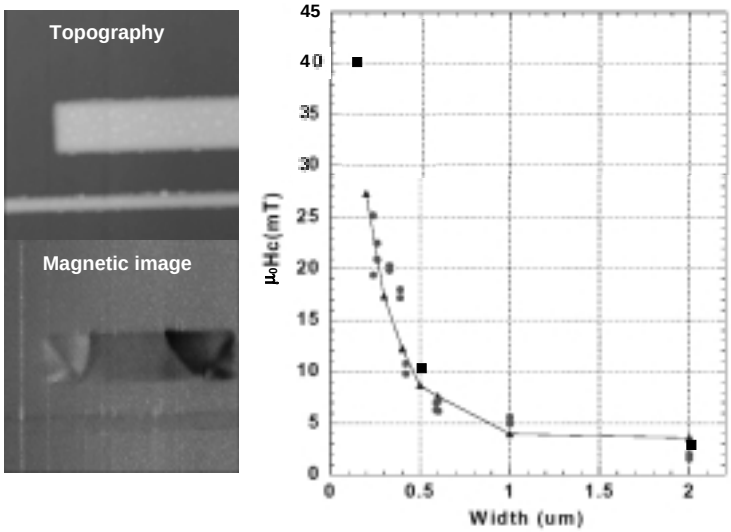

Figure 4.3: *Atomic force microscopy (AFM) and magnetic force microscopy (MFM) image (left) of* 2.0×0.5 μm^2 *and* 14.0×0.15 μm^2 *Py ferromagnetic strips. The image is taken after the Py film is deposited. The right graph shows the width dependence of the coercive magnetic field* $B_c = \mu_0 H_c$ *for mesoscopic Py strips at* $T = 4.2$ *K. The filled circles show* B_c *values of local Hall Effect (LHE) measurements (taken from [20]), the filled triangles represent a modelling of* B_c *by domain wall nucleation and solving the Landau-Lifshitz equations (taken from [20]) and the filled squares are data obtained for the Py electrodes used in this thesis. Note however that the LHE measurements are sensitive for magnetization reversal processes at the end of the Py strips, whereas in the spin injection experiments one is sensitive to the middle part of the Py strips*

sized Py strips. Coming from a negative B-field the 2.0×0.8 μm^2 electrode already has a change in the resistance before the magnetic field reaches zero. After this first drop in the resistance at -3 mT, a broad step like transition range is observed up to $+15$ mT, which indicates that the Py strip breaks up in a multiple domain structure. The amplitude of the AMR signal is about 3.3 % of the total resistance, which is a commonly reported value [1]. Although the largest part of the magnetoresistance signal is expected to originate from the AMR effect, other (smaller) contributions, such as a possible domain wall resistance cannot be excluded. The 2.0×0.5 μm^2 Py electrode shows a more 'ideal' switching behavior, showing only a resistance change after the magnetic field has crossed zero and showing a much narrower transition range from 7 to 14 mT. However, the amplitude of the resistance dip has changed to 0.7 %. Taking the minimum of the resistance dip as the switching field we find a value of 10 mT, which is much below the SW switching field of $\mu_0 H_0^{sw} =$ 65 mT. Applying the Curling model (Eq. 4.3) to calculate the curling switching field is unfortunately not al-

lowed, as the ratio d/h of this electrode is bigger than 4 ($d/h = 13$). For the narrowest strip with a width of 150 nm no magnetoresistance signal is observed in parallel field, which is an indication that this electrode behaves as a single domain or reverses its magnetization by means of a fast domain wall sweep. This hypothesis is indeed confirmed by an magnetic force microscopy (MFM) image, which is shown in Fig. 4.3. The image is taken right after the deposition of the Py film. Note that a domain structure is visible in the 2.0×0.5 μm^2 Py strip right above the 150 nm wide Py strip in Fig. 4.3.

The switching fields of the Py strips are in good agreement with results obtained by Nitta *et al.* [20], who have determined the switching fields of similar submicron Py strips by Local Hall Effect (LHE) measurements and have calculated the expected switching fields for non-uniform magnetization reversal, using the Landau-Lifshitz equation. Their results are replotted together with the results obtained for the switching fields obtained from AMR measurements of the 800 nm, 500 nm and 150 nm wide Py strips used in the injection experiments described in this thesis.

4.5 Magnetoresistance behavior of the Py/Cu contacts

A possible formation of a domain structure in the Py electrodes is important for a spin valve measurement, since the spin relaxation length of Py is very short ($\lambda \approx 5$ nm, see [21, 22]) as compared to the domain size. In case of domain formation the magnetization direction of the injecting and detecting electrodes could be determined by the local domain(s) present at the Py/Cu contact having a different magnetic switching behavior as the entire Py electrode.

Therefore local measurements of the magnetoresistance at the Py/Cu contact area are performed. These measurements are labelled with the term "contact" magnetoresistance. For example the "contact" magnetoresistance of the 14.0×0.15 μm^2 Py electrode can be measured by sending current (see Fig. 3.6 and 3.7) from contact 6 to 8 and measuring the voltage with contacts 5 and 7. Note that in this geometry one is not sensitive for a spin valve signal, as only *one* Py electrode is used in the measurement.

Fig. 4.4 shows the "contact" magnetoresistance behavior at $T = 4.2$ K of three rectangular Py electrodes with dimensions: 2.0×0.8 μm^2, 2.0×0.5 μm^2 and 14.0×0.15 μm^2. The "contact" magnetoresistance of the 500 and 800 nm wide electrodes show a similar magnetoresistance behavior as the magnetoresistance plots of the entire strips shown in Fig. 4.1, except that there seems to be more asymmetry. For the 500 nm wide electrode

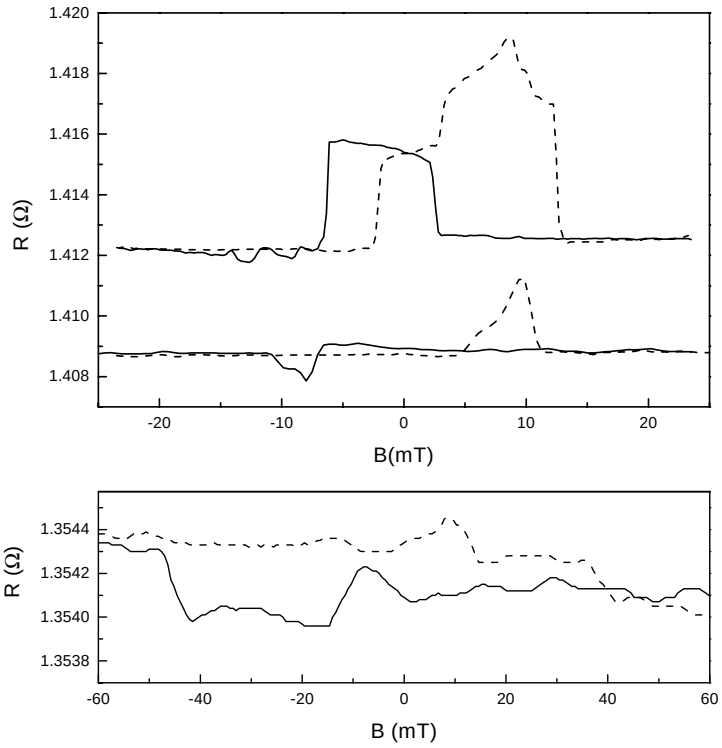

Figure 4.4: *'Contact' magnetoresistance behavior at $T = 4.2$ K of the Py/Cu contact area for Py electrodes with dimensions 2.0×0.8 μm^2 (top), 2.0×0.5 μm^2 (middle) and 14.0×0.15 μm^2(bottom). The solid (dotted) curve corresponds with a negative (positive) sweep direction of the B-field, which is applied parallel to the long (easy) axis of the Py electrode.*

a 'positive' peak is shown in the positive sweep direction and a 'negative' peak in the negative sweep direction. This indicates that the magnetization reversal process is different for a positive and negative magnetic field sweep, resulting in different domain structures at the Py/Cu contact. However, it is important to note that the amplitude of the 'contact' magnetoresistance can be as high as 7 $m\Omega$ for the 800 nm wide Py electrode. This magnitude is large compared to the amplitude of the spin valve effect, as will be shown in Chapter 5.

For the 150 nm wide Py electrode (bottom curve) a "contact" magnetoresistance behavior is observed, which appearance resembles much of a Hall signal, showing a difference in resistance at large negative and positive magnetic fields. A Hall voltage perpendicular to the substrate surface (z-direction) can be expected, as Py electrode is etched prior to the Cu deposition, causing the Cu wire to be a little bit 'sunk' into the Py electrode. Changing one voltage probe from contact 7 to contact 9 (at the other side of the Py/Cu contact area, see Fig. 3.6) produces the same signal. Also

the signal amplitude of 0.3 $m\Omega$ lies in the range of a Hall signal, which would have a maximum of 1 $m\Omega$, using a Cu Hall resistance of 1 $m\Omega/T$ for a 50 nm thick film and a maximal obtainable magnetic field change upon magnetization reversal of about 1 T. When we take the position of the Hall step as the switching field at 42 mT, also a good agreement is found with the curling switching field $\mu_0 H_c^{curl}(0°) = 40$ mT for a width $2d = 150$ nm.

References

[1] T. G. S. M. Rijks, R. Coehoorn, M. M. de Jong, and W. J. M. de Jonge, Phys. Rev. B **51**, 283 (1995).

[2] K. Hong and N. Giordano, Phys. Rev. B **51**, 9855 (1995).

[3] M. Schabes, J. Magn. Magn. Mater. **95**, 249 (1991), review article on micromagnetic theory of non-uniform magnetization processes.

[4] E. C. Stoner and E. P. Wohlfarth, Philos. Trans. London Ser. **A 240**, 599 (1948).

[5] W. F. Brown Jr., *Magnetostatic principles in ferromagnetism*, vol. 1 (North-Hollans publishing company, 1962).

[6] W. Wernsdorfer, B. Doudin, D. Mailly, K. Hasselbach, A. Benoit, J. Meier, J.-P. Ansermet, and B. Barbara, Phys. Rev. Lett. **77**, 1873 (1996).

[7] S. Pignard, G. Goglio, A. Radulescu, L. Piraux, S. Dubois, A. Declémy, and J. L. Duvail, J. Appl. Phys. **87**, 824 (2000).

[8] J.-E. Wegrowe, D. Kelly, A. Frank, S. E. Gilbert, and J.-P. Ansermet, Phys. Rev. Lett. **82**, 3681 (1999).

[9] A. Adeyeye, J. A. C. Bland, C. Daboo, J. Lee, U. Ebels, and H. Ahmed, J. Appl. Phys. **79**, 6120 (1996).

[10] A. Adeyeye, G. Lauhoff, J. A. C. Bland, C. Daboo, D. G. Hasko, and H. Ahmed, Appl. Phys. Lett. **70**, 1046 (1997).

[11] Y. Q. Jia, S. Chou, and J.-G. Zhu, J. Appl. Phys, **81**, 5461 (1997).

[12] F. G. Monzon and M. L. Roukes, J. Magn. Magn. Mater. **198**, 632 (1999).

[13] W. Brown Jr., Phys. Rev. **105**, 1479 (1957).

[14] A. Aharoni, Phys. Stat. Sol. **16** (1966).

[15] A. Aharoni, Appl. Phys. Lett. **82**, 1281 (1997).

[16] N. Smith, J. Appl. Phys. **63**, 2932 (1988).

[17] W. Wernsdorfer, K. Hasselbach, A. Sulpice, A. Benoit, J.-E. Wegrowe, L. Thomas, B. Barbara, and D. Mailly, Phys.Rev.B **53**, 3341 (1996).

[18] Y. Otani, K. Fuchamichi, O. Kitakami, Y. Shimada, B. Pannetier, J. P. Nozieres, T. Matsuda, and A. Tonomura, Proc. MRS Spring Meeting Symp. **M** (1997), San Fransisco.

[19] J. Yu, U. R*ü*diger, A. D. Kent, L. Thomas, and S. S. P. Parkin, Phys. Rev. B **60**, 7352 (1999).

[20] J. Nitta, T. Schä*p*ers, H. B. Heersche, T. Koga, Y. Sato, and H. Takayanagi, Jap. J. Appl. Phys. **41**, 2497 (2002).

[21] S. Dubois, L. Piraux, J. George, K. Ounadjela, J. Duvail, and A. Fert, Phys. Rev. B **60**, 477 (1999).

[22] S. D. Steenwyk, S. Y. Hsu, R. Loloee, J. Bass, and W. P. Pratt Jr., J. Mag. Magn. Mater. **170**, L1 (1997).